Hindawi
Journal of Nanomaterials
Volume 2019, Article ID 4139208, 14 pages
https://doi.org/10.1155/2019/4139208

Research Article

Tensile Behavior of Carbon Fiber-Reinforced Polymer Composites Incorporating Nanomaterials after Exposure to Elevated Temperature

Gia Toai Truong, Hai Van Tran, and Kyoung-Kyu Choi

School of Architecture, Soongsil Univ., 369 Sangdo–ro, Dongjak–gu, Seoul 06978, Republic of Korea

Correspondence should be addressed to Kyoung-Kyu Choi; kkchoi97@gmail.com

Received 24 July 2019; Revised 8 October 2019; Accepted 24 October 2019; Published 15 November 2019

Academic Editor: Silvia Licoccia

This study experimentally examined the effect of nanomaterial on the tensile behavior of carbon fiber-reinforced polymer (CFRP) composites. Multiwalled carbon nanotubes (MWCNT), graphene nanoplatelets (GnPs), and short multiwalled carbon nanotubes functionalized COOH (S-MWCNT-COOH) with 1% by weight were used as the primary test parameters. In the present test, S-MWCNT-COOH was more effective than the others in improving the maximum tensile strength, ultimate strain, and toughness of the CFRP composites. The use of S-MWCNT-COOH increased the maximum tensile strength, ultimate strain, and toughness of the CFRP composites by 20.7, 45.7, and 73.8%, respectively. In addition, tensile tests were carried out for CFRP composites with S-MWCNT-COOH after subjection to elevated temperatures ranging from 50 to 200°C. The test results showed that the tensile strength, ultimate strain, and toughness were significantly reduced with increasing temperature. At a temperature level of 100°C, the reduction of the maximum tensile strength, ultimate strain, and toughness was 36.5, 37.1, and 60.0%, respectively. However, for the specimens subjected to the elevated temperatures ranging from 100 to 200°C, the tensile behavioral properties were constantly maintained. Finally, various analytical models were applied to predict the tensile strength of the CFRP composites with S-MWCNT-COOH. By using the calibrated parameters, the tensile strengths predicted by the models showed good agreement with the experimental results.

1. Introduction

In recent years, fiber-reinforced polymer (FRP) composites have been widely used in the field of civil and architectural engineering as retrofitting or reinforcing material. This is due to their high strength and stiffness, low weight, and corrosion resistance [1–5]. Certainly, the development of FRP composite materials is accompanied by many challenges that must be seriously considered to achieve more extensive application of FRP materials in the construction fields. One of these challenges concerns understanding the performance of FRP materials when exposed to high temperature [6–9]. This is because once the glass transition temperature (T_g) of the epoxy matrix is approached, most FRP materials display a significant reduction of strength, stiffness, and bonding characteristics at even moderate temperature. The value of the glass transition temperature depends on the epoxy resin type but is normally in the range 60 to 82°C [10]. Moreover, when exposed to higher temperature levels of approximately 300–500°C, the adhesive material layer (organic matrices) used to fabricate FRP composites could be decomposed and even charred and thus cause deterioration of the FRPs before being subjected to load [11, 12]. Consequently, the mechanical properties of FRP composites exposed to high temperature have received continuing attention from researchers, partially because of the wide ranges of FRP materials, as well as adhesive materials.

Many studies have been experimentally carried out to investigate the effect of high temperature on the mechanical performances of FRP composites [13–21]. Obviously, the mechanical properties of the FRP composites could be characterized by tensile, compressive, flexural impact, and

interlaminar shear strength (ILSS) performances. Among them, tensile strength is one of the most basic mechanical properties of the FRP composites. This is because the FRP composites are made from fiber fabrics, which are the strongest and the most resistive to the applied load when the applied load is parallel to the fiber yarns. Therefore, most tests focused on investigating the tensile behavior of the FRP composites. For instance, Kumahara et al. [22] conducted a study on the effect of elevated temperatures on the tensile behavior of glass fiber- (GFRP) and carbon fiber- (CFRP) reinforced polymer bars and found a temperature level of 250°C, which is far beyond the glass transition temperature (T_g); GFRP and CFRP bars exhibited a tensile strength loss of over 20% compared with their original values measured at ambient temperature. Hamad et al. [23] also investigated the effect of elevated temperatures ranging from 23 to 450°C on the tensile behavior of different FRP bars. Hamad et al. [23] used high-tensile strength epoxy resin as an adhesive material. The test results showed that the FRP bars lost about 45–55% of their tensile strength and 20–30% of elastic modulus at a critical temperature of 325°C. In addition, Ashrafi et al. [24] demonstrated that the tensile behaviors of FRP materials depend not only on their type but also on their size. Among the FRP types, at a temperature of 450°C, grooved CFRP bars with vinylester resin as bonding material and GFRP bars having 10 mm diameter still retained 50% of ultimate strength at ambient temperature, while helically wrapped CFRP bars with epoxy resin as bonding material and GFRP bars having 4 mm diameter could only retain at least 50% of ultimate strength at temperature levels lower than 300 and 330°C, respectively. In general, such reduction in the strength of FRP materials is due to the visible decomposition of the epoxy resin [25]. Also, the temperature at which a FRP bar loses about half of its tensile strength is defined as the critical temperature according to the Canadian standards, CAN/CSA-S806-02 [26].

Alongside experimental studies, various analytical models have also been developed to predict the mechanical properties of FRP materials at high temperature. Based on the experimental results of Blontrock et al. [27], Saafi [28] proposed constitutive models to determine the ultimate strength and elastic modulus of various types of FRP rebars, such as aramid FRP (AFRP), CFRP, and GFRP, which decreased as temperature increased. Yu and Kodur [29] performed tensile tests on CFRP-pultruded strips and rods and fitted the obtained test results with the hyperbolic tangent function model by modifying the model of Gibson et al. [30]. Bai and Keller [31] also proposed a general model with the parameters based on dynamic mechanical analysis (DMA) results. The model by Bai and Keller [31] could be applied for the shear, tensile, and compressive strengths of FRP materials. In general, each model could display good agreement with its own experimental results. To use such models for various FRP composites at high temperature, relevant studies are needed.

Recently, many studies exhibited good enhancement in mechanical properties of the FRP composites when adding nanomaterials into adhesive matrix [1–3, 32]. Zhou et al. [1] examined the effect of carbon nanofibers (CNF) on the flexural, tensile, and fatigue behaviors of satin weave carbon fabric composites. With 2% CNF by weight (2 wt.%), it was reported that the flexural strength and tensile strength increased by 22.3 and 11%, respectively. In addition, the improvement in fatigue performance of the CFRP composites was observed. Srivastava et al. [32] investigated mode I and mode II fracture toughness of CFRP composites using double-cantilever beam (DCB) and end-notched flexure (ENF) tests. The obtained test results indicated that the use of graphene nanoplatelets (GnPs) could result in higher fracture toughness in mode I and interlaminar shear strength (ILSS) than MWCNTs and carbon blacks (CBs). Meanwhile, MWCNTs could produce higher fracture toughness in mode II than the others.

In this study, the effect of incorporating nanomaterials on the tensile behavior of carbon fiber-reinforced polymer (CFRP) composites was experimentally investigated. Three different nanomaterial types, namely, multiwalled carbon nanotubes (MWCNTs), graphene nanoplatelets (GnPs), and short multiwalled carbon nanotubes functionalized COOH (S-MWCNT-COOH), were utilized. The FRP composites are widely used for strengthening concrete structures including infrastructures, but they show poor material performance under high temperature. Thus, understanding the materials' characteristics at high temperature of the FRP composites is very important. In addition, since the experimental data on the tensile properties of the FRP composites with nanomaterials exposed to elevated temperature are limited, this study also examined the tensile properties of the CFRP composites with S-MWCNT-COOH after exposure to the elevated temperatures ranging from 50 to 200°C. This investigation is necessary to safely and reliably use the CFRP composites as building materials. Finally, various analytical models were applied to predict the tensile strength of CFRP composites with S-MWCNT-COOH after exposure to elevated temperatures.

2. Experimental Program

2.1. Material Properties. Carbon fiber fabrics T300-3000 consisting of 3k filaments and having a thickness of 0.21 mm were used as reinforcement materials. The average density and weight of the carbon fiber fabrics were 1.76 g/cm^3 and 0.198 g/m, respectively. The tensile strength, elastic modulus, and ultimate tensile strain of the carbon fiber fabrics were 3,530 MPa, 230,000 MPa, and 1.5%, respectively, as given by the manufacturer. Figure 1 presents the carbon fiber fabric used in this study.

Three types of nanomaterial (or nanoparticles) of multiwalled carbon nanotubes (MWCNTs), graphene nanoplatelets (GnPs), and short multiwalled carbon nanotubes functionalized COOH (S-MWCNT-COOH) were used as nanofillers (Korea Nanomaterials, Gyeonggi-do, Korea). The use of such three nanomaterials has been consistently considered by researchers due to their widely commercial availability and low cost compared to the others, such as single-walled CNTs, double-walled CNTs, and xGnP. Figure 2 presents the nanomaterials used in this study. In the figure, the GnP nanoparticle could be easily distinguished from the others by eye based on its gray color, while

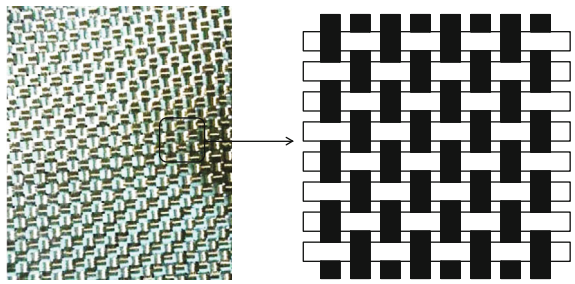

(a) (b)

Figure 1: Carbon fiber fabric used in this study. (a) Photo of carbon fiber fabric. (b) Plain weave of carbon fiber fabric.

(a) MWCNTs (b) S-MWCNT-COOH

(c) GnPs

Figure 2: Nanomaterials used in this study.

MWCNT and S-MWCNT-COOH nanoparticles were black. In general, these nanoparticles were manufactured by high technology with purity over 90 wt.%. In addition, each nanoparticle type was different from the others in terms of length, diameter, and surface area. Table 1 details the geometries and properties of these nanoparticles.

The epoxy resin used in this study as an adhesive material is a Bisphenol-A type liquid diluted with butyl glycidyl ether (BGE). The epoxy has excellent properties, such as good adhesive strength, chemical resistance after curing, high reactivity, and low viscosity. The viscosity of this epoxy is about 800 to 1,600 cps at 25°C. Such low viscosity allows it to bind carbon fiber fabrics well during the fabrication process. A corresponding polyamidoamine hardener was used and has a low viscosity with a value ranging from 500 to 1,000 cps at 25°C. The stoichiometric ratio between epoxy and hardener was 100 : 55 by weight.

2.2. Test Specimens of Carbon Fiber-Reinforced Polymer (CFRP) Composites. Figure 3 details the CFRP test specimens. The figure shows that the CFRP test specimens were of 250 mm length and 25 mm width. The length of the CFRP specimen included gripping zones at two ends and a central zone for measuring the deformation of the specimen. The length of the gripping zone was 50 mm, and that of the central zone was 150 mm. At the gripping zone of the test specimens, carbon fiber-reinforced polymer (CFRP) tabs were used to avoid slippage between test specimens and the clamping grips of the universal testing machine (UTM) during the tensile test and to ensure that the failure of the test specimens occurred within the central zone.

Table 1: Geometry and properties of nanomaterials.

Nanomaterials	Carbon purity (wt.%)	Sizes
Multiwalled carbon nanotubes (MWCNTs)	>95	Outside diameter: 10–20 nm Inside diameter: 5–10 nm Length: 10–30 μm Specific surface area > 200 m^2/g Density: 2.1 g/cm^3
Graphene nanoplatelets (GnPs)	>90	Average number of layers < 30 Median size (diameter): 5–7 μm Density: 2.25 g/cm^3
Short multiwalled carbon nanotubes functionalized COOH (S-MWCNT-COOH)	>90	Outside diameter: 30–50 nm Inside diameter: 5–12 nm Length: 0.5–2 μm Specific surface area > 60 m^2/g Density: 2.1 g/cm^3

In this study, twenty-four test specimens were fabricated to experimentally investigate the effects of nanomaterial type and elevated temperature on the tensile performance of carbon fiber-reinforced polymer (CFRP) composites. In the first test series, three types of CFRP test specimens were prepared by incorporating MWCNT, S-MWCNT-COOH, and GnP nanomaterials. To distinguish these test specimens, the test specimens were named MWCNT-CFRP, S-MWCNT-COOH-CFRP, and GnPs-CFRP. Each test specimen was made as three replicates. These test specimens were cured at experimental room temperature (RT; approximately 18°C) for 48 h before testing.

The second test series was carried out to study the effects of high temperature on the tensile behavior of the CFRP composites with nanomaterials. The test results obtained from the first series showed that the use of S-MWCNT-COOH could result in higher peak strength and ultimate strain of the CFRP composites than other nanomaterials. Thus, in this study, the performance of

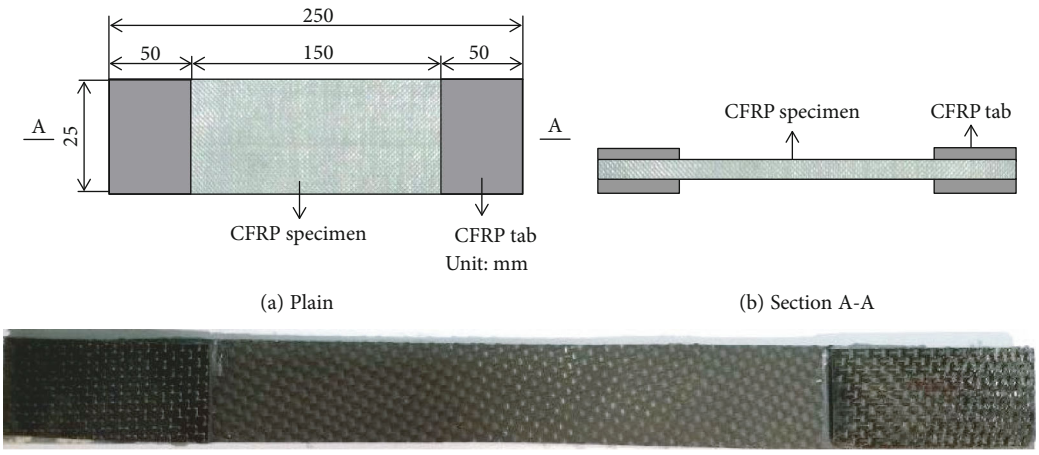

Figure 3: Details of the test specimens.

the CFRP composites with S-MWCNT-COOH after exposure to high temperature would be strictly tested and investigated. In the second test series, all test specimens had the same configurations and amount of S-MWCNT-COOH nanoparticle, while the applied temperature varied from 50 to 200°C. Also, the five types of test specimens were first cured at RT condition for 48 h and then exposed to different temperature levels of 50, 100, 150, and 200°C for 2 h in an electric heating furnace. The elevated temperature range was limited to 200°C to avoid the rapid decomposition and burning of the epoxy resin. This is similar to the temperature ranges applied in the studies by Cao et al. [33] and Chowdhury et al. [34]. Meanwhile, the exposure time is determined based on the studies by Bazli et al. [12], Li et al. [14], and Ellis et al. [16]. After heating for two hours, the test specimens were naturally cooled down prior to direct tensile test. To distinguish the CFRP composite specimens with and without exposure to high temperature, the number indicating the temperature of the specimens was added to specimen names. For example, the specimen of S-MWCNT-COOH-T50 was subjected to a temperature level of 50°C. For each test parameter, three duplicates of the test specimens were prepared for reliable results.

2.3. Fabrication of Epoxy-NT Nanocomposite. In this study, prior to fabrication of the CFRP composites, the epoxy resin and nanomaterial (NT) mixtures were prepared. For control specimens of CFRP composites, the carbon fiber fabrics were impregnated by the pure epoxy (without the nanomaterial). The pure epoxy mixture was prepared by mixing epoxy resin with the hardener.

In the cases of the other CFRP composites, the carbon fiber fabrics were impregnated by the treated epoxies. Such treated epoxies were prepared by dispersing nanomaterials (MWCNTs, GnPs, and S-MWCNT-COOH) on the epoxy resin. The amounts of MWCNTs, GnPs, and S-MWCNT-COOH used in this test were 1% by weight. For the first type, after adding the amount of MWCNTs into the epoxy resin as required, the mixture was sonicated by a sonicator machine for 1 h at 40°C. The use of higher temperature during the sonication (40°C compared to 25°C) is to reduce the epoxy resin viscosity, which could result in more effective dispersion of multiwalled carbon nanotubes in the epoxy resin [35]. Then, the hardener was added into the mixture of epoxy resin and MWCNTs and mechanically stirred, to form epoxy-MWCNT nanocomposites. Finally, the epoxy-MWCNT nanocomposites were coated on the surface of carbon fiber fabrics.

For the second type, the GnP dispersion on the epoxy resin was performed by using a sonicator for 45 min at RT. Afterwards, the dispersed epoxy-GnP mixture was degassed in a vacuum oven for 15 min at 40°C to remove air bubbles and any sediment of solvent [36]. Subsequently, the hardener was added into the epoxy-GnP mixture, and the epoxy-GnP nanocomposites were steadily stirred and coated on the surface of carbon fiber fabrics.

The third type was produced by adding S-MWCNTs-COOH into the pure epoxy resin, and then, the mixture was sonicated by a sonicator machine for 1 h at 40°C to ensure dispersion of S-MWCNTs-COOH in the epoxy. However, to efficiently mix epoxy and S-MWCNT-COOH, the mixture was stirred for 30 min at 80°C. According to Soliman et al. [35], this was to enhance the chemical reaction between the functional groups (COOH) on the surface of nanotubes and the resin chains. Subsequently, the epoxy-S-MWCNTs-COOH mixture was naturally cooled down to RT. Afterwards, the hardener was added into the mixture, mechanically stirred to form epoxy-S-MWCNTs-COOH nanocomposites, and then used to fabricate CFRP composites.

2.4. Fabrication of Test Specimens. In this study, the hand layup method was applied to fabricate CFRP composite test specimens, due to its ease and simplification. The carbon fiber fabrics having dimensions of 300 mm × 100 mm (length × width) were prepared to make the CFRP composite plates. Two carbon fiber layers were used to fabricate the composite specimens. The acrylic plates were used as mold to ensure the stretch of the composite specimens. Before starting the layup process, the mold was coated with a

releasing agent to avoid the composite specimens adhering to the mold. The carbon fiber fabrics were coated with epoxy-NT nanocomposites on two surfaces and placed on the mold following the required stacking sequences. The epoxy-NT nanocomposites were impregnated into the carbon fiber fabrics by brush. The same weight ratio between epoxy-NT composites and carbon fiber fabrics was used to ensure the same epoxy weight fraction, as well as the amount of nanoparticles (1% by weight) in epoxy resin. The epoxy weight fraction was determined by the difference of carbon fiber fabrics before and after impregnation with epoxy. In this study, the epoxy weight ratio was approximately 54%. Finally, the CFRP specimens were cured at RT (approximately 18°C) for 48 h in the experimental room under an applied load of 250 N. Subsequently, the specimens in the second series were exposed to high temperature of 50, 100, 150, and 200°C for 2 h in the electric heating furnace. Figure 4 presents the electric heating furnace used in this study. The electric heating furnace has a heating capacity of over 900°C and has internal dimensions of 300 mm × 300 mm × 600 mm (width × height × length). The completed composite plates were then carved up into the test specimens to execute the tensile testing (Figure 3).

2.5. Test Setup. The direct tensile test was performed following the guidance specified in test standard KS M ISO 527-4 [37], with a testing velocity of 0.5 mm/min. Figure 5 details the direct test setup used for the CFRP composite specimens. In the figure, a universal testing machine (UTM) having a load capacity of 1,000 kN was utilized to perform the tensile test. An extensometer, with 50 mm gauge length, was used to measure the deformation of the test specimens (Figure 5).

3. Test Results and Discussions

3.1. Failure Modes of the CFRP Composites. Figure 6(a) presents the failure modes of the CFRP composites incorporating nanomaterial. In the figure, the pure CFRP composite exhibited brittle failure at a single cross-section, and the test specimen was completely separated. The CFRP composites incorporating MWCNTs, GnPs, and S-MWCNT-COOH displayed a similar failure mode. This means that the use of a particular nanomaterial did not affect the failure mode of the CFRP composites.

Figure 6(b) shows the failure mode of the CFRP composites with 1 wt.% of S-MWCNT-COOH after exposure to elevated temperatures. In general, the failure mode of S-MWCNT-COOH-CFRP specimens was not affected by the temperature. Under different temperature levels, the test specimens were still characterized by brittle failure. This is attributed to the effective bonding performance between the nanophased epoxy and fibers, even at high temperatures.

3.2. Effect of Various Nanomaterials on the Tensile Behavior of CFRP Composites. Figure 7 shows the stress-strain relationships of the CFRP composites incorporating various types of nanomaterial of MWCNTs, GnPs, and S-MWCNT-COOH, in comparison with those of the pure CFRP composites. It can be seen that the CFRP composites with and without nanomaterials exhibited a slight fluctuation of stress-strain response. However, such fluctuation was not considerable and the stress-strain responses of the CFRPs showed a linear relationship at early loading stage. The slope of the stress-strain curves is determined as the initial stiffness (E, or elastic modulus) of the CFRP specimens [38]. In this study, the elastic modulus is determined by dividing the stress at 30% of the peak strength in the ascending branch by the corresponding strain. Also, the other mechanical parameters of maximum tensile strength (σ_u) and ultimate strain (ε_u) were computed and are presented in Table 2. In this study, the tensile stress was determined by dividing the applied load by the nominal cross-sectional area of the test specimens, which is equal to the nominal thickness of two layers of CFRP composites (2 × 0.21 mm) multiplied by the width of specimens (25 mm) [34]. The ultimate strain of test specimens was defined as the maximum strain at failure because the specimens showed a sudden drop after reaching the maximum tensile strength. In addition, tensile toughness (or toughness), which indicates the ability of the material to absorb energy before failure, was also determined by calculating the area under the stress-strain curve, and Table 2 also presents the obtained values.

In general, the figure indicates that after reaching the maximum tensile strength, all test specimens failed in brittle mode with a sudden drop. In addition, it was found from the figure that the addition of nanomaterial could partially improve the tensile strength and ultimate strain of the CFRP composites. This confirms that the nanomaterial was not agglomerated during mixing and formed with uniform dispersion, which caused the enhanced tensile properties of the CFRP composites. The addition of 1 wt.% nanomaterials into epoxy resin is reasonable. Such uniform dispersion of nanomaterials created better interlocking performance between the fiber fabrics and matrix, which plays an important role in arresting the development of cracks in the epoxy matrix, and thus enhanced the load-carrying capacity of the CFRP composite during tensile loading [39, 40].

Figure 8 shows a detailed comparison of the CFRP composites. Figure 8(a) shows that the initial stiffness of the composites incorporating nanomaterial showed a slight reduction compared to that of the pure CFRP composites. Similar behavior was also observed in the study by Soliman et al. [35]. Nevertheless, the stiffness reduction due to the addition of nanoparticles needs to be investigated further. In the case of MWCNT-CFRP specimens, the tensile strength (Figure 8(b)), ultimate strain (Figure 8(c)), and toughness (Figure 8(d)) were increased by 7.4, 20.2, and 27.6%, compared to those of the pure CFRP. The increase of toughness was owing to the stress transfer capacity of nanomaterial from matrix to fiber fabrics by the interlocking system after cracking of the matrix. This enhanced the ability to absorb energy of the CFRP composites incorporating nanomaterial. The GnPs-CFPRP specimens showed an increase in the ultimate strain and toughness by approximately 13.6 and 11.9%, respectively, even though the maximum tensile strength was not increased. The S-MWCNT-COOH-CFRP specimens showed a significant increase in the maximum tensile strength, ultimate strain, and toughness by 22.8, 46.6, and

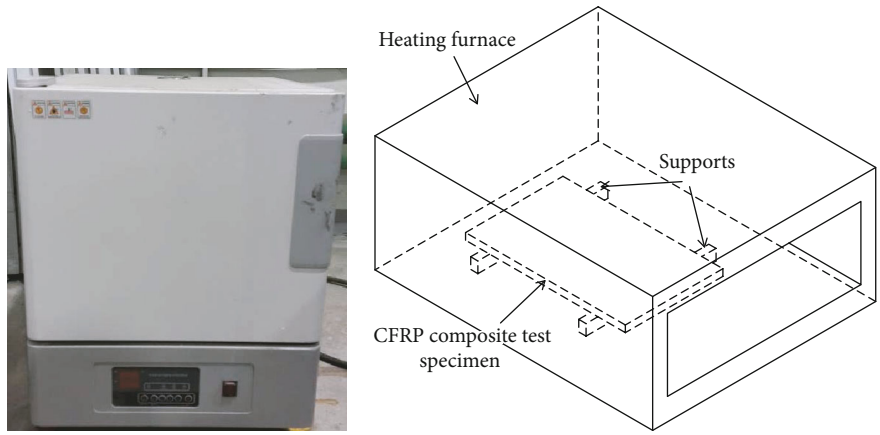

(a) Photo of electric heating furnace (b) Illustration of heating setup

Figure 4: Heating test setup.

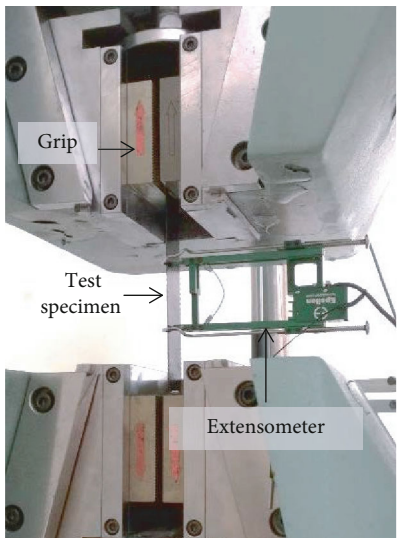

Figure 5: Direct tensile test setup.

77.8%, respectively, compared with the pure CFRP. In the present study, the use of S-MWCNT-COOH produced the most effective enhancement in the tensile properties of the CFRP composites. The COOH functional groups affixed to short MWCNTs significantly increased the bond performance at the interfacial zone between nanotubes and epoxy resin and thus improved the tensile behaviors of the CFRP composites [41]. Meanwhile, the GnPs exhibited less improvement than the others, which may be due to the low strength of the GnPs used in this study.

3.3. Effect of Temperature on the Tensile Behavior of CFRP Composites. Figure 9 presents the stress-strain responses of the test specimens in the S-MWCNT-COOH-CFRP series after exposure to high temperature. In general, the shape of stress-strain curves at high-temperature levels ranging from 50 to 200°C was similar to that at RT (18°C). From the figure, it is obvious that after exposure to high temperature, the S-MWCNT-COOH-CFRP specimens exhibited a significant reduction of tensile strength and ultimate strain.

Figure 10 presents the variation of mechanical parameters of the S-MWCNT-COOH-CFRP composites, including their initial stiffness, maximum tensile strength, ultimate strain, and toughness according to the applied temperature. Figure 10(a) shows that the initial stiffness of S-MWCNT-COOH-CFRP specimens was almost the same, regardless of the applied temperature. In the studies by Alsayed et al. [25] and Correia et al. [42], a similar phenomenon for initial stiffness was observed. Note that in the studies by Alsayed et al. [25] and Correia et al. [42], the tensile test results were performed for GFRP bars and pultruded materials, respectively. The fact indicates that high temperature might not considerably affect the stiffness of S-MWCNT-COOH-CFRP. Nevertheless, further research is necessary to confirm this investigation.

Figure 10 shows that the maximum tensile strength, ultimate strain, and toughness displayed the same decreasing trend according to the applied temperature. Up to the temperature level of 100°C, the S-MWCNT-COOH-CFRP specimens showed steep reductions in maximum tensile strength, ultimate strain, and toughness. At 100°C, the maximum tensile strength reduced about 36.5%, and the ultimate strain and toughness showed reductions of 37.1 and 60.0%, respectively. After that, at higher temperature levels beyond 100°C, the maximum tensile strength, ultimate strain, and toughness were almost constant. The reduction of such mechanical properties of the composites was attributed to the softening of epoxy at high-temperature levels, which reduced the interaction and the stress transfer capacity between fiber fabrics. However, different from the pure epoxy, the nanomaterials were not severely damaged, even in high temperature. Thus, the epoxy with nanomaterials could partially maintain the stress transfer capacity between fiber fabrics. Because of the effect, the composites could maintain their mechanical properties at a temperature level up to 200°C [33, 34, 42]. The obtained test results also indicated that at a temperature level of 200°C, the S-MWCNT-COOH-CFRP composite could retain at least 66.7% of

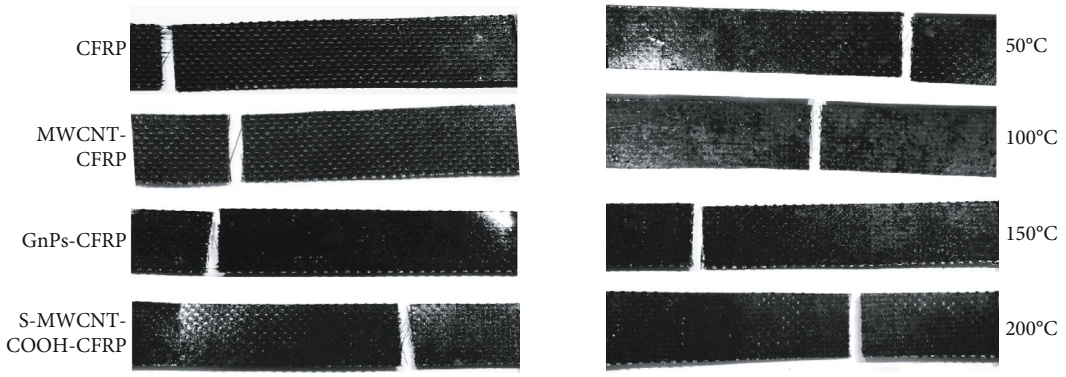

(a) Effect of nanomaterials (b) Effect of temperatures on S-MWCNT-COOH-CFRP specimens

Figure 6: Failure patterns of CFRP composites.

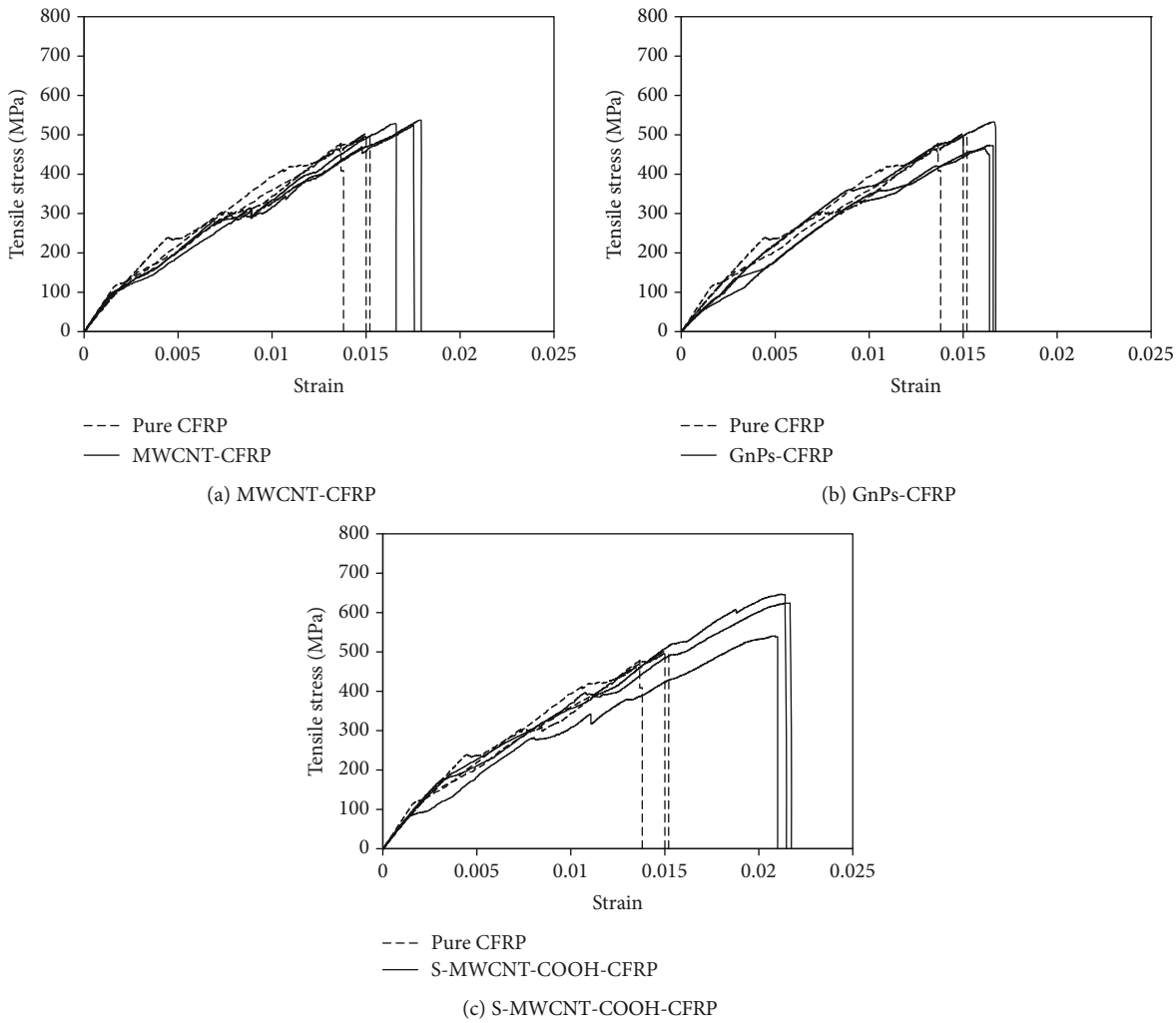

(a) MWCNT-CFRP (b) GnPs-CFRP

(c) S-MWCNT-COOH-CFRP

Figure 7: Stress-strain curves of the CFRP composites incorporating nanomaterial.

maximum tensile strength, 61.6% of ultimate strain, and 41.0% of toughness, compared to those at RT (18°C). According to CAN/CSA-S806-02 [26], the critical temperature corresponding to 50% strength reduction is suggested apart from the glass transition temperature T_g. Thus, it could be expected that based on CAN/CSA-S806-02, S-MWCNT-COOH composites have a critical temperature higher than 200°C [26].

3.4. Prediction Models for the CFRP Specimens Exposed to High Temperature. In the previous studies [43–46], thermal-mechanical models have been developed to predict

Table 2: Tensile test results of the CFRP test specimens.

Specimens	Mechanical parameters							
	E^1 (GPa)	SD[2]	σ_u (MPa)	SD	ε_u	SD	Toughness (MPa·mm/mm)	SD
CFRP	53.34	4.30	492.32	12.45	0.0144	0.00082	3.60	0.28
MWCNT-CFRP	41.55	2.32	528.69	6.42	0.0174	0.00068	4.59	0.22
GnPs-CFRP	41.87	5.89	490.31	36.32	0.0164	0.00027	4.02	0.36
S-MWCNT-COOH-CFRP	44.98	8.40	604.35	55.95	0.0212	0.00027	6.40	0.66
S-MWCNT-COOH-CFRP-T50	42.54	5.71	502.17	40.92	0.0190	0.00155	4.80	0.72
S-MWCNT-COOH-CFRP-T100	47.74	7.22	383.87	32.86	0.0133	0.00091	2.56	0.32
S-MWCNT-COOH-CFRP-T150	50.43	8.74	417.77	39.54	0.0144	0.00067	3.02	0.39
S-MWCNT-COOH-CFRP-T200	44.77	10.30	403.18	13.03	0.0130	0.00087	2.62	0.16

[1]Initial stiffness (or elastic modulus) at 30% of the peak strength in the ascending branch. [2]Standard deviation.

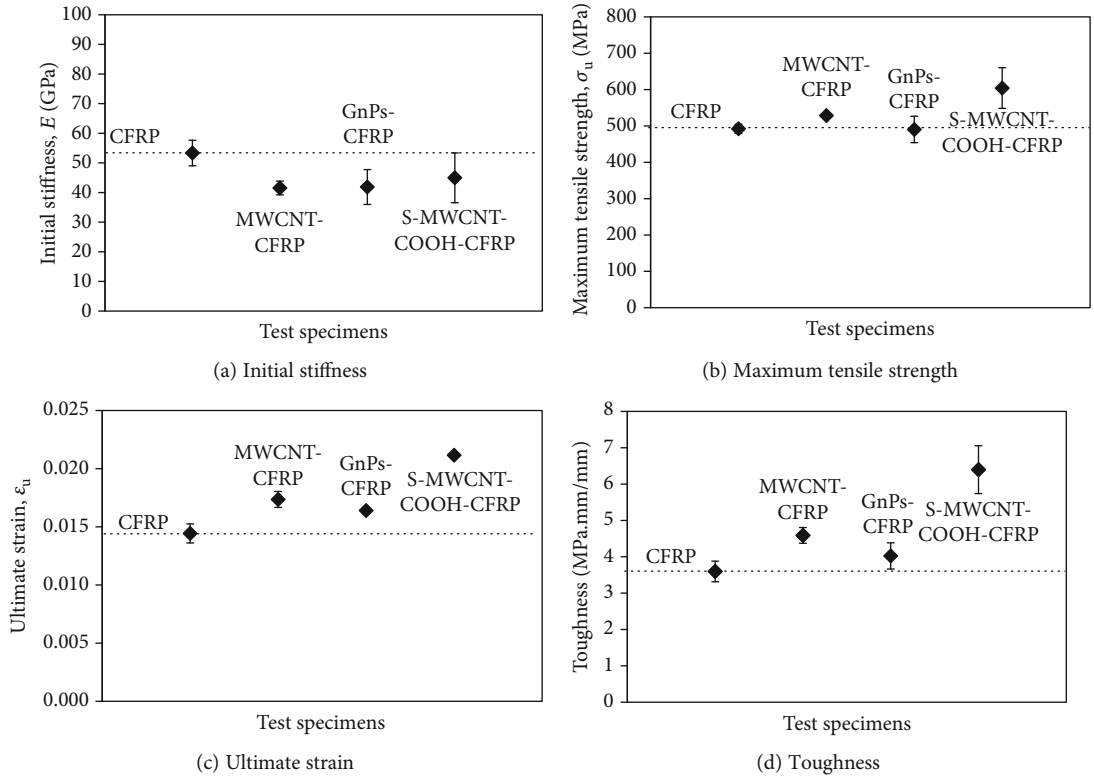

(a) Initial stiffness (b) Maximum tensile strength

(c) Ultimate strain (d) Toughness

Figure 8: Effect of various nanomaterials on the tensile properties of CFRP composites.

the temperature, decomposition, softening, mechanical properties, and failure of the FRP composites during firing, as well as the models to calculate the postfire properties of the FRP composites (after exposure to high temperature). In this study, to predict the tensile strength of S-MWCNT-COOH-CFRP specimens after exposure to high temperature, the existing models of Gibson et al. [30], Bisby [47], Mahieux et al. [48], and Wang et al. [49] were used, by calibrating the parameters based on the test results. Note that these models were originally developed to predict the tensile strength of FRP composites at high temperature (from ambient temperature to 700°C).

3.4.1. Prediction by the Gibson et al. Model [30]. Gibson et al. [30] proposed an empirical curve-fitting equation in the form of a hyperbolic tangent function to fit the test data considering the effect of high temperature.

$$f(T) = R^n \left\{ \frac{f_o + f_p}{2} - \frac{f_o - f_p}{2} \tanh\left[\mu(T - T_s)\right] \right\}, \quad (1)$$

where $f(T)$ is the tensile strength at temperature T; f_o is the tensile strength at RT; f_p is the tensile strength at high temperature; μ is the coefficient considering the effect of temperature; T_s is the mechanical temperature of CFRP composites, which is determined at the point where the tensile strength-temperature curve is nearly symmetrical; R is the residual resin content considering the effect of high

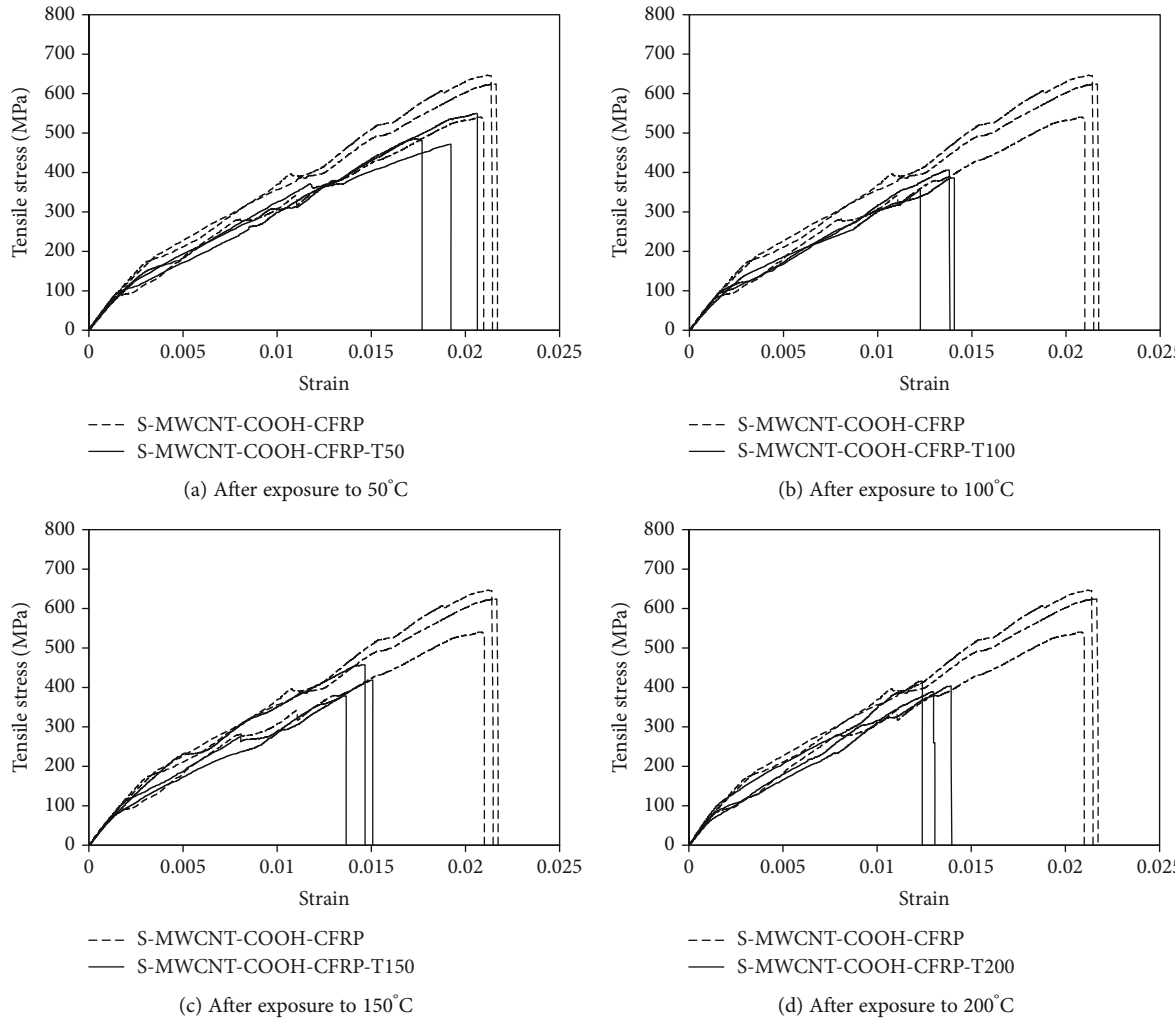

Figure 9: Stress-strain curves of the CFRP composites with S-MWCNT-COOH after exposure to elevated temperature.

temperature (between 0 and 1); and n is a parameter that depends on the stress state of CFRP composites.

In the present study, based on the test results, $f_o = 604.35$ MPa at RT (approximately 18°C) and $f_p = 383.87$ MPa at 100°C were determined. In addition, μ was determined by fitting the experimental data; a constant value of μ (0.04) was used for $18 \le T \le 200$°C. T_s was determined to be 55°C. In the case of R, under high temperature, the resin content could be reduced [47]. However, in this study, R was assumed to be 1 for all test specimens. Finally, $n = 0$ was used, because the carbon fiber fabrics mainly governed the failure mode of the CFRP composites.

Figure 11(a) presents the tensile strength–temperature curve from the experiment and the model for S-MWCNT-COOH-CFRP specimens. The figure shows that the tensile strength–temperature curve predicted by the Gibson et al. model was in reasonable agreement with the experimental curve.

3.4.2. Prediction by the Bisby Model [47]. Bisby [47] proposed the following semiempirical sigmoid function to describe the reductions in FRP mechanical properties with temperature:

$$f(T) = f_o\left[\left(\frac{1-a}{2}\right)\tanh\{-b(T-c)\} + \left(\frac{1+a}{2}\right)\right], \quad (2)$$

where a, b, and c are empirically derived coefficients. Based on the existing database of experimental data on various FRP products, Bisby [46] derived the coefficients for the tensile strength of carbon fiber-reinforced polymer (CFRP) and glass fiber-reinforced polymer (GFRP) materials at high temperature, as presented in Table 3.

Figure 11(b) presents the relationship between tensile strength and temperature obtained from the experimental results and the prediction by the Bisby model. The figure indicates that the prediction values of tensile strength using the original coefficients proposed by Bisby for CFRP were significantly different from the experimental results. This is inevitable, because the FRP material used in this study was carbon fiber-reinforced polymer composite incorporating short multiwalled carbon nanotubes functionalized COOH (S-MWCNT-COOH-CFRP), which is very different from

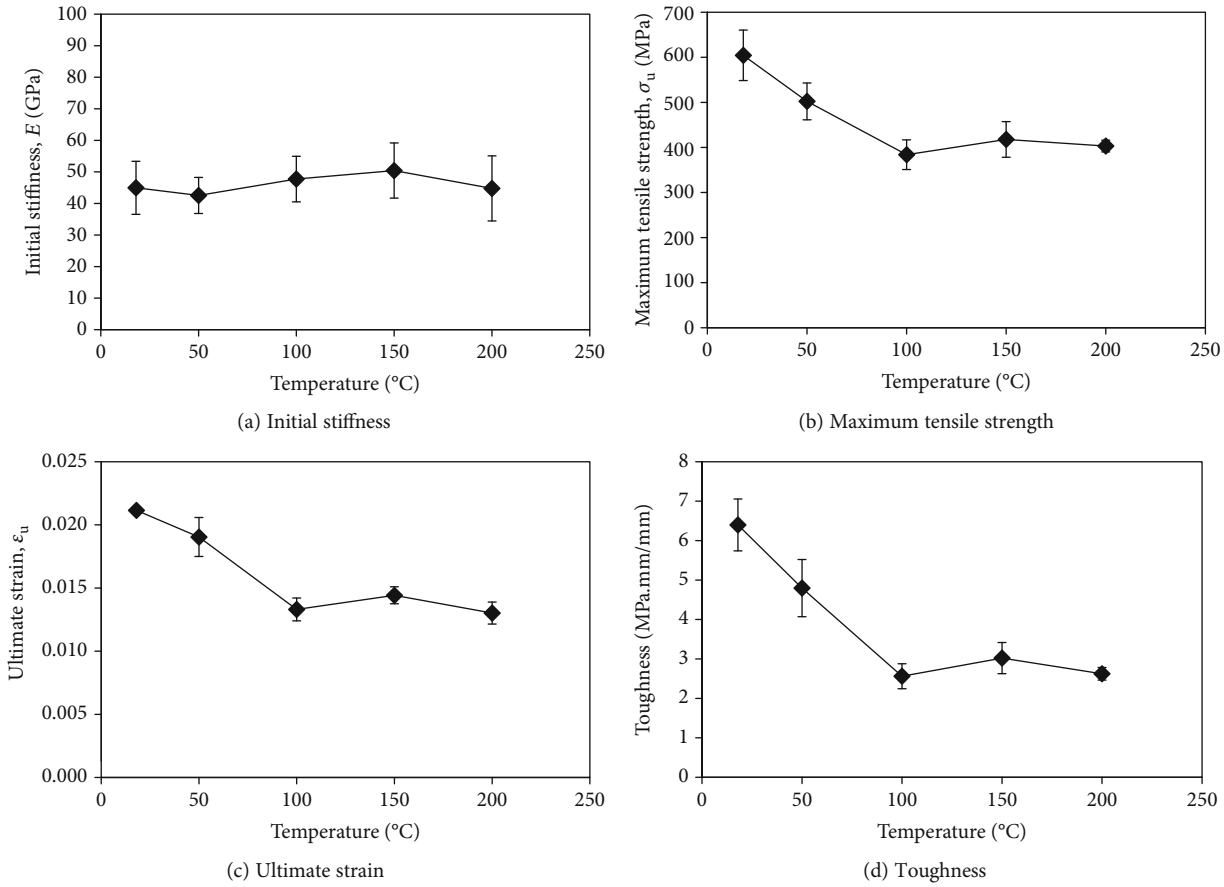

Figure 10: Effect of temperature on the tensile properties of CFRP composites with S-MWCNT-COOH.

the pure CFRP. Based on the present study, a modification to the coefficient c is proposed. However, the other coefficients of $a = 0.1$ and $b = 0.00583$ originally suggested by Bisby for CFRP were used in this study. Table 4 presents the coefficient c calibrated with the experimental data for different temperature ranges: $c = 370 - 4T$, $210 - 0.8T$, and $50 + T$ for $18 \le T \le 50^{\circ}\text{C}$, $50 \le T \le 100^{\circ}\text{C}$, and $100 \le T \le 200^{\circ}\text{C}$, respectively. By using the calibrated coefficient c, the tensile strength–temperature curve predicted by the Bisby model was in good agreement with the experimental results, as shown in Figure 11(b).

3.4.3. Prediction by the Mahieux et al. Model [48]. Mahieux et al. [48] suggested the following functional relationship based on the Weibull distribution to calculate the strength as a function of temperature (in Kelvin):

$$f(T) = f_{\text{p}} + \left(f_{\text{o}} - f_{\text{p}}\right) \exp\left[-\left(\frac{T}{T_{\text{s}}}\right)^{m}\right], \tag{3}$$

where m is the Weibull exponent obtained by fitting the experimental data.

In this study, the model developed by Mahieux et al. [48] was applied to predict the evolution of the tensile strength of S-MWCNT-COOH-CFRP composites according to temperature. Based on the present test results, $f_{\text{p}} = 383.87$ MPa, $f_{\text{o}} = 604.35$ MPa, and $T_{\text{s}} = 55^{\circ}\text{C}$ (321.15 in Kelvin) were determined. The coefficient m to fit the experimental data was determined to be 29.12. Figure 11(c) indicates that the prediction curve of the tensile strength versus temperature was in good agreement with the experimental results.

3.4.4. Prediction by the Wang et al. Model [49]. Wang et al. [49] originally developed a prediction model for metal and applied it to evaluate the tensile strength of CFRP-pultruded strips at high temperature with some calibrated parameters:

$$f(T) = f_{\text{o}}\left[A - \frac{(T - B)^{n}}{C}\right], \tag{4}$$

where A, B, C, and n are coefficients calibrated for different temperature ranges and are presented in Table 5.

In this study, $f_o = 604.35$ MPa is the tensile strength at RT (approximately 18°C). The lower limit of the coefficient B was modified to 18, which was equal to the RT of the test specimens.

In general, as shown in Figure 11(d), by using the parameters proposed by Wang et al. [49], which were originally used for CFRP-pultruded strips, the predicted tensile strength–temperature curve showed slight differences from the experimental results. Hence, a modification of the coefficients A, C, and n the corresponding temperature range was

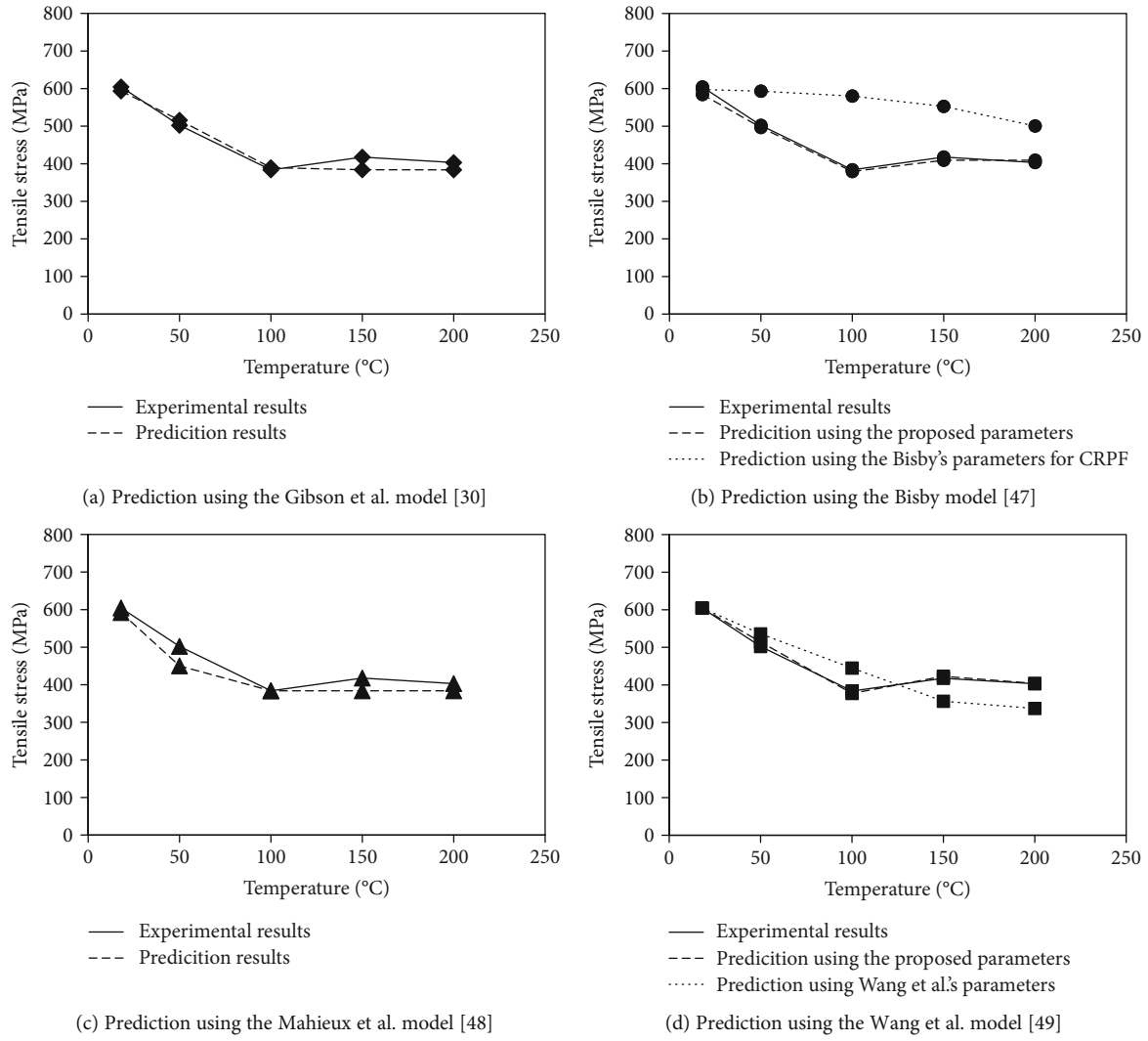

(a) Prediction using the Gibson et al. model [30]

(b) Prediction using the Bisby model [47]

(c) Prediction using the Mahieux et al. model [48]

(d) Prediction using the Wang et al. model [49]

Figure 11: Prediction of the tensile strength of CFRP composites after exposure to elevated temperature.

Table 3: Coefficients for tensile strength suggested by Bisby [47].

Material	Coefficients		
	a	b	c
CFRP	0.10	0.00583	339.54

Table 4: Proposed coefficients for use in the Bisby model [47] for the tensile strength of S-MWCNT-COOH-CFRP specimens at elevated temperature.

Temperature range (°C)	Coefficients		
	a	b	c
$18 \le T \le 50$	0.10	0.00583	$370 - 4T$
$50 \le T \le 100$			$210 - 0.8T$
$100 \le T \le 200$			$50 + T$

proposed, as presented in Table 6. With such modifications, the prediction curve was close to the experimental results (see Figure 11(d)).

3.4.5. Performance Evaluation of the Models. In this study, to evaluate the efficiency of the models in predicting CFRP composites with 1 wt.% of S-MWCNT-COOH after exposure to elevated temperature, two indices of the root-mean-squared error (RMSE) and the coefficient of determination (R^2) would be calculated.

The root mean squared error is an index to evaluate the goodness of prediction to verify the experimental results. This index is computed by measuring the difference between the predicted values and the experimental values, as shown in Equation (5):

$$\mathrm{RMSE} = \sqrt{\frac{\sum_{i=1}^{n}\left(y_{i,\mathrm{ex}} - y_{i,\mathrm{pre}}\right)^2}{n}}. \quad (5)$$

The coefficient of determination (R^2) is calculated as

Table 5: Coefficients for tensile strength suggested by Wang et al. [49].

Temperature range (°C)	Coefficients			
	A	B	C	n
$22 \le T < 150$	1.00	22	200	0.9
$150 \le T < 420$	0.59	150	490	0.7

Table 6: Proposed coefficients for use in the Wang et al. model [49] for the tensile strength of S-MWCNT-COOH-CFRP specimens at elevated temperature.

Temperature range (°C)	Coefficients			
	A	B	C	n
$18 \le T \le 100$	1.00	18	200	0.98
$100 \le T \le 150$	1.00	18	$4T - 200$	0.98
$150 \le T \le 200$	0.73	150	490	0.7

Table 7: RMSE and R^2 values for the various prediction models.

Properties	Models			
	Gibson et al. [30]	Bisby [47]	Mahieux et al. [48]	Wang et al. [49]
RMSE	19.255	10.567	29.505	6.521
R^2	0.944	0.983	0.870	0.94

expressed in Equation (6). The R^2 values range from 0 to 1, and the higher R^2 indicates the greater usefulness of the model:

$$R^2 = 1 - \frac{\sum_{i=1}^{n} \left(y_{i,\text{ex}} - y_{i,\text{pre}}\right)^2}{\sum_{i=1}^{n} \left(y_{i,\text{ex}} - \bar{y}\right)^2}, \quad (6)$$

where $y_{i,\text{ex}}$ is the experimental value, $y_{i,\text{pre}}$ is the corresponding predicted value, $\bar{y}$ is the average of the experimental values, and n is the number of samples.

Table 7 presents the values of RMSE and R^2 that were computed for all models. In general, all models fit well the prediction of the experimental data, because the values of R^2 are close to 1. For a given test data, the model of Wang et al. [49] is more efficient than the others, since the RMSE value (6.521) was the lowest.

4. Conclusions

This study investigated the effect of nanomaterial on the tensile behavior of CFRP composites. Three different types of nanomaterial of MWCNT, GnPs, and S-MWCNT-COOH were investigated. Significant enhancements in the tensile strength, ultimate strength, and toughness of CFRP composites were observed. Among the nanomaterial used, S-MWCNT-COOH was the most effective by increasing the maximum tensile strength, ultimate strain, and toughness by 20.7, 45.7, and 73.8%, respectively.

From the obtained test results, the tensile behaviors of S-MWCNT-COOH-CFRP composites subjected to elevated temperatures ranging from 50 to 200°C were also tested and compared to those at RT (18°C). The test results showed that tensile strength, ultimate strain, and toughness were reduced with increasing temperature. At 100°C, the reduction of maximum tensile strength, ultimate strain, and toughness was 36.5, 37.1, and 60.0%, respectively. However, at temperature levels higher than 100°C, the mechanical properties of the composites were almost stable.

Various analytical models were applied to predict the tensile strength of CFRP composites with 1 wt% of S-MWCNT-COOH. With calibrated parameters corresponding to the temperature ranges, most models could predict the tensile strength of the carbon fiber-reinforced polymer composites incorporating short multiwalled nanotubes functionalized COOH with good accuracy.

Data Availability

The tensile test data used to support the findings of this study are included within the article.

Conflicts of Interest

The authors declare that they have no conflicts of interest.

Acknowledgments

This research was supported by the Basic Science Research Program through the National Research Foundation of Korea (NRF) funded by the Ministry of Education (No. 2017R1D1A1B04033611).

References

[1] Y. Zhou, F. Pervin, S. Jeelani, and P. K. Mallick, "Improvement in mechanical properties of carbon fabric–epoxy composite using carbon nanofibers," *Journal of Materials Processing Technology*, vol. 198, no. 1-3, pp. 445–453, 2008.

[2] N. G. Ozdemir, T. Zhang, I. Aspin, F. Scarpa, H. Hadavinia, and Y. Song, "Toughening of carbon fibre reinforced polymer composites with rubber nanoparticles for advanced industrial applications," *Express Polymer Letters*, vol. 10, no. 5, pp. 394–407, 2016.

[3] Z. Dai, F. Shi, B. Zhang, M. Li, and Z. Zhang, "Effect of sizing on carbon fiber surface properties and fibers/epoxy interfacial adhesion," *Applied Surface Science*, vol. 257, no. 15, pp. 6980–6985, 2011.

[4] H. Wang, H. Memon, E. A. M. Hassan, M. S. Miah, and M. A. Ali, "Effect of jute fiber modification on mechanical properties of jute fiber composite," *Materials*, vol. 12, no. 8, p. 1226, 2019.

[5] A. Caggiano, "Machining of fibre reinforced plastic composite materials," *Materials*, vol. 11, no. 3, p. 442, 2018.

[6] V. K. R. Kodur, L. A. Bisby, and S. H. C. Foo, "Thermal behavior of fire-exposed concrete slabs reinforced with fiber-reinforced polymer bars," *ACI Structural Journal*, vol. 102, no. 6, pp. 799–807, 2005.

[7] F. Zhou, J. Zhang, S. Song, D. Yang, and C. Wang, "Effect of temperature on material properties of carbon fiber reinforced

polymer (CFRP) tendons: experiments and model assessment," *Materials*, vol. 12, no. 7, p. 1025, 2019.

[8] M. Robert and B. Benmokrane, "Behavior of GFRP reinforcing bars subjected to extreme temperatures," *Journal of Composite Construction*, vol. 14, no. 4, pp. 353–360, 2009.

[9] M. Frigione and M. Lettieri, "Durability issues and challenges for material advancements in FRP employed in the construction industry," *Polymers*, vol. 10, no. 3, p. 247, 2018.

[10] ACI 440 2R-08, *Guide for the Design and Construction of Externally Bonded FRP Systems for Strengthening Concrete Structures*, ACI Committee 440, Farmington Hills, MI, USA, 2008.

[11] J. R. Correia, F. A. Branco, and J. G. Ferreira, "The effect of different passive fire protection systems on the fire reaction properties of GFRP pultruded profiles for civil construction," *Composites Part A: Applied Science and Manufacturing*, vol. 41, no. 3, pp. 441–452, 2010.

[12] M. Bazli, H. Ashrafi, A. Jafari, X.-L. Zhao, H. Gholipour, and A. V. Oskouei, "Effect of thickness and reinforcement configuration on flexural and impact behaviour of GFRP laminates after exposure to elevated temperatures," *Composites Part B: Engineering*, vol. 157, pp. 76–99, 2019.

[13] Y.-J. Hu, C. Jiang, W. Liu, Q.-Q. Yu, and Y.-L. Zhou, "Degradation of the in-plane shear modulus of structural BFRP laminates due to high temperature," *Sensors*, vol. 18, no. 10, p. 3361, 2018.

[14] G. Li, J. Zhao, and Z. Wang, "Fatigue behavior of glass fiber-reinforced polymer bars after elevated temperatures exposure," *Materials*, vol. 11, no. 6, p. 1028, 2018.

[15] C. Li, G. Xian, and H. Li, "Water absorption and distribution in a pultruded unidirectional carbon/glass hybrid rod under hydraulic pressure and elevated temperatures," *Polymers*, vol. 10, no. 6, p. 627, 2018.

[16] D. Ellis, H. Tabatabai, and A. Nabizadeh, "Residual tensile strength and bond properties of GFRP bars after exposure to elevated temperatures," *Materials*, vol. 11, no. 3, p. 346, 2018.

[17] Z. Lu, G. Xian, and K. Rashid, "Creep behavior of resin matrix and basalt fiber reinforced polymer (BFRP) plate at elevated temperatures," *Journal of Composites Science*, vol. 1, no. 1, p. 3, 2017.

[18] I. Garcia-Moreno, M. A. Caminero, G. P. Rodriguez, and J. J. Lopez-Cela, "Effect of thermal ageing on the impact damage resistance and tolerance of carbon-fibre-reinforced epoxy laminates," *Polymers*, vol. 11, no. 1, p. 160, 2019.

[19] G. Terrasi, E. McIntyre, L. Bisby, T. Lämmlein, and P. Lura, "Transient thermal tensile behaviour of novel pitch-based ultra-high modulus CFRP tendons," *Polymers*, vol. 8, no. 12, p. 446, 2016.

[20] L. A. Bisby, M. F. Green, and V. K. R. Kodur, "Response to fire of concrete structures that incorporate FRP," *Progress in Structural Engineering and Materials*, vol. 7, no. 3, pp. 136–149, 2005.

[21] C.-H. Shen and G. S. Springer, "Effects of moisture and temperature on the tensile strength of composite materials," *Journal of Composite Materials*, vol. 11, no. 1, pp. 2–16, 1977.

[22] S. Kumahara, Y. Masuda, and Y. Tanao, "Tensile strength of continuous fiber bar under high temperature," *International Concrete Abstracts Portal*, vol. 138, pp. 731–742, 1993.

[23] R. J. A. Hamad, M. A. Megat Johari, and R. H. Haddad, "Mechanical properties and bond characteristics of different fiber reinforced polymer rebars at elevated temperatures," *Construction and Building Materials*, vol. 142, pp. 521–535, 2017.

[24] H. Ashrafi, M. Bazli, E. P. Najafabadi, and A. Vatani Oskouei, "The effect of mechanical and thermal properties of FRP bars on their tensile performance under elevated temperatures," *Construction and Building Materials*, vol. 157, pp. 1001–1010, 2017.

[25] S. Alsayed, Y. al-Salloum, T. Almusallam, S. el-Gamal, and M. Aqel, "Performance of glass fiber reinforced polymer bars under elevated temperatures," *Composites Part B: Engineering*, vol. 43, no. 5, pp. 2265–2271, 2012.

[26] C. S. CAN, *CSA-S806-02, Design and Construction Building Components with Fibre-Reinforced Polymers*, Canadian Standards Association, Mississauga, ON, Canada, 2002.

[27] H. Blontrock, L. Taerwe, and S. Mathys, "Properties of fiber reinforced plastics at elevated temperature with regard to fire resistance of reinforced concrete members," in *Fourth International Symposium on Non-Metallic (FRP) Reinforced for Concrete Structures*, pp. 43–54, American Concrete Institute (ACI), Baltimore, MD, USA, 1999.

[28] M. Saafi, "Effect of fire on FRP reinforced concrete members," *Composite Structures*, vol. 58, no. 1, pp. 11–20, 2002.

[29] B. Yu and V. Kodur, "Effect of temperature on strength and stiffness properties of near-surface mounted FRP reinforcement," *Composites Part B: Engineering*, vol. 58, pp. 510–517, 2014.

[30] A. G. Gibson, Y. . S. Wu, J. T. Evans, and A. P. Mouritz, "Laminate theory analysis of composites under load in fire," *Journal of Composite Materials*, vol. 40, no. 7, pp. 639–658, 2006.

[31] Y. Bai and T. Keller, "Modeling of strength degradation for fiber-reinforced polymer composites in fire," *Journal of Composite Materials*, vol. 43, no. 21, pp. 2371–2385, 2009.

[32] V. K. Srivastava, T. Gries, D. Veit, T. Quadflieg, B. Mohr, and M. Kolloch, "Effect of nanomaterial on mode I and mode II interlaminar fracture toughness of woven carbon fabric reinforced polymer composites," *Engineering Fracture Mechanics*, vol. 180, pp. 73–86, 2017.

[33] S. Cao, Z. Wu, and X. Wang, "Tensile properties of CFRP and hybrid FRP composites at elevated temperatures," *Journal of Composite Materials*, vol. 43, no. 4, pp. 315–330, 2009.

[34] E. U. Chowdhury, R. Eedson, L. A. Bisby, M. F. Green, and N. Benichou, "Mechanical characterization of fibre reinforced polymers materials at high temperature," *Fire Technology*, vol. 47, no. 4, pp. 1063–1080, 2011.

[35] E. Soliman, M. Al-Haik, and M. R. Taha, "On and off-axis tension behavior of fiber reinforced polymer composites incorporating multi-walled carbon nanotubes," *Journal of Composite Materials*, vol. 46, no. 14, pp. 1661–1675, 2011.

[36] S. Chatterjee, F. Nafezarefi, N. H. Tai, L. Schlagenhauf, F. A. Nuesch, and B. T. T. Chu, "Size and synergy effects of nanofiller hybrids including graphene nanoplatelets and carbon nanotubes in mechanical properties of epoxy composites," *Carbon*, vol. 50, no. 15, pp. 5380–5386, 2012.

[37] KS M ISO 527-4, *Plastics – Determination of Tensile Properties – Part 4: Test Conditions for Isotropic and Orthotropic Fibre – Reinforced Plastic Composites*, Korean Standard Association, 2012.

[38] M. Yadav, K. Y. Rhee, I. H. Jung, and S. J. Park, "Eco-friendly synthesis, characterization and properties of a sodium carboxymethyl cellulose/graphene oxide nanocomposite film," *Cellulose*, vol. 20, no. 2, pp. 687–698, 2013.

[39] M. K. Hossain, M. M. R. Chowdhury, M. B. A. Salam et al., "Enhanced mechanical properties of carbon fiber/epoxy composites by incorporating XD-grade carbon nanotube," *Journal of Composite Materials*, vol. 49, no. 18, pp. 2251–2263, 2015.

[40] F. Tariq, M. Shifa, and R. A. Baloch, "Mechanical and thermal properties of multi-scale carbon Nanotubes–Carbon fiber–epoxy composite," *Arabian Journal for Science and Engineering*, vol. 43, no. 11, pp. 5937–5948, 2018.

[41] E. Soliman, U. Kandil, and M. Taha, "Improved strength and toughness of carbon woven fabric composites with functionalized MWCNTs," *Materials*, vol. 7, no. 6, pp. 4640–4657, 2014.

[42] J. R. Correia, M. M. Gomes, J. M. Pires, and F. A. Branco, "Mechanical behaviour of pultruded glass fibre reinforced polymer composites at elevated temperature: experiments and model assessment," *Composite Structures*, vol. 98, pp. 303–313, 2013.

[43] C. A. Griffis, J. A. Nemes, F. R. Stonesifer, and C. I. Chang, "Degradation in strength of laminated composites subjected to intense heating and mechanical loading," *Journal of Composite Materials*, vol. 20, no. 3, pp. 216–235, 1986.

[44] G. A. Pering, P. V. Farrell, and G. S. Springer, "Degradation of tensile and shear properties of composites exposed to fire or high temperature," *Journal of Composite Materials*, vol. 14, no. 1, pp. 54–66, 1980.

[45] S. Feih, Z. Mathys, A. G. Gibson, and A. P. Mouritz, "Modelling the tension and compression strengths of polymer laminates in fire," *Composites Science and Technology*, vol. 67, no. 3-4, pp. 551–564, 2007.

[46] A. P. Mouritz and Z. Mathys, "Post-fire mechanical properties of glass-reinforced polyester composites," *Composites Science and Technology*, vol. 61, no. 4, pp. 475–490, 2001.

[47] L. A. Bisby, *Fire Behavior of Fibre-Reinforced Polymer (FRP) Reinforced or Confined Concrete, [Ph.D. thesis]*, Queen University, Kingston, ON, Canada, 2003.

[48] C. A. Mahieux, K. L. Reifsnider, and S. W. Case, "Property Modeling across Transition Temperatures in PMC's: Part I. Tensile Properties," *Applied Composite Materials*, vol. 8, no. 4, pp. 217–234, 2001.

[49] K. Wang, B. Young, and S. T. Smith, "Mechanical properties of pultruded carbon fibre-reinforced polymer (CFRP) plates at elevated temperatures," *Engineering Structures*, vol. 33, no. 7, pp. 2154–2161, 2011.